On the stochastic uncertainties of thermally and optically stimulated luminescence signals

Pagonis, Vasilis; Kreutzer, Sebastian; Duncan, Alex Roy; Rajovic, Ena; Laag, Christian; Schmidt, Christoph

Published in:
Journal of Luminescence

DOI:
10.1016/j.jlumin.2019.116945

Publication date:
2020

Citation for published version (APA):
Pagonis, V., Kreutzer, S., Duncan, A. R., Rajovic, E., Laag, C., & Schmidt, C. (2020). On the stochastic uncertainties of thermally and optically stimulated luminescence signals: A Monte Carlo approach. *Journal of Luminescence*, *219*, 116945. Article 116945. https://doi.org/10.1016/j.jlumin.2019.116945

On the stochastic uncertainties of thermally and optically stimulated luminescence signals: A Monte Carlo approach

Vasilis Pagonis*[,a], Sebastian Kreutzer[b], Alex Roy Duncan[c], Ena Rajovic[c], Christian Laag[c,d], Christoph Schmidt[c]

[a] *McDaniel College, Physics Department, Westminster, MD 21157, USA*
[b] *IRAMAT-CRP2A, UMR 5060 CNRS - Université Bordeaux Montaigne, Maison de l'Archéologie, Esplande des Antilles, 33607 Pessac Cedex, France*
[c] *Chair of Geomorphology, University of Bayreuth, 95440 Bayreuth, Germany*
[d] *Université de Paris, Institut de Physique du Globe de Paris, CNRS, F-75005 Paris, France*

Abstract

Phenomenological models are frequently used to analyze experimental signals in thermally and optically stimulated luminescence experiments. Typically, these models consist of systems of differential equations describing various electronic transitions. An alternative to the differential equation approach is the use of Monte Carlo (MC) methods, which also allow an estimation of the theoretical stochastic uncertainty of the intensity of the luminescence signal. By running and averaging several MC variants, these stochastic uncertainties are estimated in this paper for various luminescence models.

In the case of first-order kinetics processes, the MC results compare well with previously published analytical results for the coefficient of variation (CV) in stochastic linear pure death processes. By contrast, no analytical results are available for the more general one trap one recombination center model (OTOR), and MC is the only method available for estimating the stochastic uncertainties.

In this paper the CV coefficients are simulated for three commonly used experimental stimulation modes, namely thermally stimulated luminescence (TL), continuous wave optically stimulated luminescence (CW-OSL) and linearly modulated OSL (LM-OSL). The results of the simulations show that CW-OSL signals have the smallest CV values among the three stimulation modes, and therefore these signals are least likely to exhibit stochastic variations. The stochastic uncertainties in these phenomenological models are discussed in the context of single grain luminescence experiments and nanodosimetric materials, in which one deals with small numbers of charge carriers.

Key words: birth and death stochastic processes, Monte Carlo method,

*Corresponding author
Email address: vpagonis@mcdaniel.edu (Vasilis Pagonis)

Thermoluminescence, Optically Stimulated Luminescence, Infra - red stimulated Luminescence

---

1. Introduction

Phenomenological models are frequently used to analyze experimental signals in stimulated luminescence experiments. Within these phenomenological models, various experimental stimulation methods are commonly used in the laboratory. Specifically thermal stimulation produces thermoluminescence (TL) signals , while optical stimulation with visible light produces optically stimulated luminescence (OSL). For a review of the models commonly used to describe these signals, the readers are referred to several available excellent textbooks and review articles on luminescence dosimetry and its applications (Chen and McKeever [1], McKeever and Chen [2], Bøtter-Jensen et al. [3], Pagonis et al. [4], Chen and Pagonis [5], Yukihara and McKeever [6], Kitis et al. [7]).

Typically, phenomenological luminescence models consist of systems of differential equations describing various electronic transitions. In most cases, these equations must be solved numerically using appropriate initial conditions, while analytical solutions have been developed for some of the simpler models.

An alternative to the differential equations approach in these phenomenological models, is the use of Monte Carlo (MC) methods. One of the main advantages of the MC approach is that it can be applied to systems consisting of a very small number of charge carriers, in which the luminescence signals may be different from the corresponding signals in bulk materials. An additional advantage is that MC can also produce estimates of the stochastic uncertainties in luminescence signals, by running and averaging several MC variants. These stochastic uncertainties can only be obtained with the MC approach, and can become important for nanodosimetric materials, in which one deals with small clusters of spatially correlated defects (traps and centers). Monte-Carlo methods for the study of TL were presented for example in the papers by Mandowski and Świątek [8], Mandowski [9, 10, 11], Kulkarni [12], Pagonis et al. [13]. The stochastic nature of TL phenomena was the subject of two papers by Swandic [14, 15], who examined the so called master equations in a luminescence model of simultaneous irradiation and heating of a sample.

However, these previous MC simulation studies did not address in any detail the *stochastic uncertainties* in the phenomenological models used to describe thermally and optically stimulated luminescence signals.

Our motivation for the present MC study stems from recently published experimental and modeling results on luminescence signals from nanodosimetric materials (Polymeris et al., [16]), and also from single grain luminescence modeling and experiments (Autzen et al. [17]. The relevance of the MC simulations in this paper for these two research areas is considered in the Discussion and Conclusions.

This paper presents simulations of several phenomenological luminescence models, by

using the MC method recently used in Pagonis et al. [13]. Specifically, the MC method is used to estimate the *stochastic* theoretical uncertainty of the population of trapped electrons, and of the luminescence intensity in the various models.

The overall purpose of the paper is to obtain estimates of these stochastic uncertainties, which are introduced by the randomness of the luminescence processes in small clusters of traps and centers.

The specific goals of the paper are:

- To apply the MC method of Pagonis et al. [13] to several well-known luminescence models, and to simulate various types of TL and OSL experiments within these luminescence models.
- To obtain a quantitative estimate of the stochastic uncertainties for both the populations of trapped electrons, and for the intensity of the luminescence signal.
- To compare the stochastic uncertainties of various types of TL and OSL experiments.
- Where possible, to compare the stochastic uncertainties from the MC method, with available analytical expressions previously derived for stochastic birth and death processes (Novozhilov et al. [18]).

This paper is organized as follows. Section 2 is a general overview of various luminescence signals measured in the laboratory, and their basic mathematical foundation. Section 3 provides a general discussion and summarizes previously published equations for the stochastic uncertainties in linear birth and death stochastic processes.

Section 4 describes the general MC method used in this paper, and is followed in Section 5.1 by simulations of first-order TL, linear modulated OSL (LM-OSL) and isothermal TL (ITL) kinetic processes. In Section 5.2 we present results for the GOT/OTOR model, which is the simplest delocalized phenomenological model in luminescence studies. The paper concludes with a general discussion of the results, within the context of single grain luminescence experiments and nanodosimetric materials.

2. Experimental stimulation modes and phenomenological models for stimulated luminescence phenomena

In this section we present an overview of several phenomenological models used to describe stimulated luminescence phenomena. In addition, this section also summarizes three thermal and optical stimulation modes which are commonly used in luminescence experiments. Both the models and the various stimulation modes are simulated in this paper.

The models summarized here are collectively described as first-order luminescence kinetics models. In addition, we also summarize the simplest luminescence model of one trap and one recombination center model (OTOR). As discussed for example recently in the review paper by Kitis et al. [7], the differential equations describing thermally and optically stimulated phenomena contain the function $p(t)$ which represents the stimulation rate.

When the sample is thermally stimulated, the stimulated luminescence signal is called *Thermoluminescence* (TL), and the function $p(t)$ is given by:

$$p(t) = s\, e^{-\frac{E}{kT(t)}} \tag{1}$$

where E (eV) is the thermal activation energy of the trap, and s (s^{-1}) is the associated frequency factor, k (eV/K) is the Boltzmann constant and $T(t)$ (K) is the temperature of the sample at time $t(s)$. The differential equation for first-order TL kinetics is the well-known Randall-Wilkins equation [19]:

$$\frac{dn}{dt} = -s\, e^{-\frac{E}{kT(t)}}\, n \tag{2}$$

where n (m^{-3}) is the concentration of trapped electrons at time t. The function $T(t)$ describes the variation of the temperature T with time t, during the TL experiment. In most TL experiments, one uses a constant heating rate β (K/s), such that $T(t) = T_0 + \beta t$, where T_o is the initial temperature of the heating process.

When the thermal stimulation takes place at a constant temperature T_{ISO}, the stimulated luminescence signal is called *isothermal luminescence* (ITL), and the function $p(t)$ is given by:

$$p(t) = s\, e^{-\frac{E}{kT_{ISO}}} \tag{3}$$

and the corresponding differential equation for first-order processes is:

$$\frac{dn}{dt} = -s\, e^{-\frac{E}{kT_{ISO}}}\, n \tag{4}$$

When the stimulation is optical in nature using visible light of constant intensity, the stimulated luminescence is termed *continuous wave optically stimulated luminescence* (CW-OSL). In this case the function $p(t)$ is given by:

$$p(t) = \sigma\, I \tag{5}$$

where σ (cm^2) represents the optical cross section for the CW-OSL process, and I $(photons\, cm^{-2}\, s^{-1})$ represents the photon flux. The corresponding differential equation for first-order CW-OSL

processes is:

$$\frac{dn}{dt} = -A_{CW}\, n \tag{6}$$

where $A_{CW} = \sigma\, I$. When the optical stimulation takes place using a source with a linearly varying intensity, the stimulated luminescence is called *linearly modulated optically stimulated luminescence* (LM-OSL) and the function $p(t)$ is given by Bulur [20]:

$$p(t) = \frac{\sigma\, I}{P}\, t = \frac{A_{LM}}{P}\, t \tag{7}$$

where σ, I have the same meaning as in Eq.5, $P\,(s)$ is the total illumination time, and $A_{LM} = \sigma\, I$. The corresponding differential equation for first-order LM-OSL processes is:

$$\frac{dn}{dt} = -\frac{A_{LM}}{P}\, t\, n \tag{8}$$

The most common and simplest phenomenological energy band model is the OTOR model, shown as a schematic energy diagram in Fig.1. The arrows indicate the delocalized transitions in the model, which can also describe retrapping of the electrons during the thermal/optical excitation of the sample. By using the quasi-equilibrium (QE) assumption in which the free electron concentration in the conduction band is quasi-stationary (Chen and McKeever [1]), the OTOR model leads to the following general one trap (GOT) differential equation:

$$I(t) = -\frac{dn}{dt} = p(t)\, \frac{n^2}{(N-n)R + n}. \tag{9}$$

Here $n(m^{-3})$ is the concentration of electrons in traps, and N is the total concentration of trapping states. The dimensionless quantity R is called the *retrapping ratio*, and is defined as:

$$R = A_n / A_m \tag{10}$$

where $A_n(cm^3 s^{-1})$ is the retrapping coefficient of electrons, and $A_m(cm^3 s^{-1})$ the recombination coefficient of electrons. The GOT equation was first introduced by Adirovitch [21] and Halperin and Braner [22], and its analytical solution was obtained close to 50 years later by Kitis and Vlachos [23] by using the Lambert W-function. This model leads to first and second order kinetics for certain values of the parameters in the model, as discussed in the recent review paper by Kitis et al. [7]. For example, when retrapping processes can be neglected the OTOR model leads to first order kinetics, while the case of second order kinetics is obtained when the coefficients of retrapping and recombination are equal ($A_n = A_m$).

3. Stimulated luminescence as a stochastic process

3.1. Stochastic uncertainties for the population of electrons

The *deterministic* differential equations for TL, ITL, CW-OSL and LM-OSL processes described in the previous section, can be written in the general form:

$$\frac{dn}{dt} = -\mu(t)\, n. \tag{11}$$

where the rate parameter $\mu(t)$ is either a constant μ independent of the time t (as in the cases of ITL and CW-OSL experiments), or an explicit function of time $\mu(t)$ (as in the cases of TL and LM-OSL experiments).

This type of differential equation is closely associated with *stochastic* processes, known as birth and death processes (see for example Krishnan [24]). Birth-death processes have been studied within the context of continuous-time Markov processes, and they have been applied to diverse areas of science. For example, they have been used widely in the study of epidemics, in the description of biological/physiological systems , in queuing theory etc. Novozhilov et al. [18]. However, to the best of our knowledge, there have been no previous studies of birth and death processes within the context of TL and OSL phenomena.

A stochastic birth and death process is such that only two types of state transitions are present, births and deaths. In a birth transition, the state variable of the system increases by one, while in a death process the state decreases by one. In very general terms, in a stochastic birth-death process one considers an appropriately small time Δt, in which only three types of transitions can take place: one death, or one birth, or no birth/death. The probabilities of these three transitions are $\lambda\Delta t$, $\mu\Delta t$ and $1-(\lambda+\mu)\Delta t$ where λ (s^{-1}) is the rate of birth events and μ (s^{-1}) is the rate of death events $(\lambda, \mu > 0)$. When $\lambda = 0$ and $\mu \neq 0$, one is dealing with *pure death processes*, which are the subject of this section.

When the death rate is μ =constant (as in the ITL and CW-OSL phenomena), the *mean* $< n >$ and the *variance* σ_n^2 of the population of remaining electrons are given by the following equations (see for example Allen [25], p.254, Table 6.1):

$$< n >= n_o p = n_o e^{-\mu\, t}\,, \tag{12}$$

$$\sigma_n^2 =< n^2 > - < n >^2 = n_o pq = n_o e^{-\mu\, t}\left(1 - e^{-\mu\, t}\right) \tag{13}$$

where n_o is the initial number of trapped electrons at time $t = 0$. By combining Eqts.(12)

and (13), we find the dimensionless *coefficient of variation* (CV), expressed in %:

$$CV[\%] = 100\frac{\sigma_n}{< n >} = 100\frac{\sqrt{n_o e^{-\mu\, t}\,(1 - e^{-\mu\, t})}}{n_o e^{-\mu\, t}} = 100\sqrt{\frac{e^{\mu\, t} - 1}{n_o}} \tag{14}$$

When the death rate parameter $\mu(t)$ is an explicit function of time (as in the cases of TL and LM-OSL stimulation modes), the *mean* $< n >$ and the *variance* σ_n^2 of the population of trapped electrons is given by the following equations (see Kendall [26], Eqts.13,14):

$$< n >= n_o \exp(-\int_0^t \mu(t')dt') \tag{15}$$

$$\sigma_n^2 = n_o \left[\exp(-\int_0^t \mu(t')dt') - \exp(-2\int_0^t \mu(t')dt')\right] \tag{16}$$

and the $CV[\%]$ in this more general case of $\mu(t) \neq$ constant, is given by:

$$CV[\%] = 100\frac{\sigma_n}{< n >} = 100\sqrt{\frac{e^{\int_0^t \mu(t')dt'} - 1}{n_o}} \tag{17}$$

When $\mu(t) = \mu =$ constant, the last three equations revert to the previous three simpler equations (12) , (13) and (14). In the case of TL, the death rate is $\mu(t) = s\, exp\,[-E/(kT)]$ and the integral is $\int_0^t \mu(t')dt'$ is evaluated numerically during the simulations in this paper. In the case of LM-OSL, the death rate is $\mu(t) = \sigma\, I\, t/P$, and the integral is $\int_0^t \mu(t')dt' = \sigma\, I\, t^2/(2P)$.

3.2. Calculation of the variance σ_L^2 of the luminescence intensity

The equations discussed in Section 3.1, describe the mean $< n >$ and the variance σ_n^2 of the population of trapped electrons. From an experimental point of view, we are also interested in the variance σ_L^2 of the luminescence intensity L.

This quantity σ_L^2 can be evaluated from:

$$\sigma_L^2 =< \left(\frac{dn}{dt}\right)^2 > - < \frac{dn}{dt} >^2 \tag{18}$$

By using Eqt.(11):

$$\sigma_L^2 =< (\mu(t)\, n)^2 > - < \mu(t)\, n >^2 = \mu(t)^2 \left(< n^2 > - < n >^2\right) = \mu(t)^2\, \sigma_n^2 \tag{19}$$

$$\sigma_L = \mu(t)\, \sigma_n \tag{20}$$

In the case of TL,

$$\sigma_{TL} = \left(s\, e^{-\frac{E}{kT(t)}} \right) \sigma_n \tag{21}$$

In the case of LM-OSL,

$$\sigma_{LMOSL} = \left(\frac{\sigma\, I}{P}\, t \right) \sigma_n \tag{22}$$

In the cases of ITL and CW-OSL,

$$\sigma_{ISO} = \left(s\, e^{-\frac{E}{kT_{ISO}}} \right) \sigma_n \quad \text{and} \quad \sigma_{CWOSL}{=}(\sigma I)\ \sigma_n \tag{23}$$

respectively. It is clear that in ITL and CW-OSL experiments, the variance of the luminescence signal σ_L^2 is directly proportional to the variance σ_n^2 of the population of filled traps. However, in the case of TL and LM-OSL experiments we can expect that the two variances σ_L^2, σ_n^2 will have a different dependence on time (or temperature).

4. General description of the MC method

The basic Monte Carlo technique of solving differential equations is found in many standard textbooks of simulations in Statistical Physics (see for example [27];[28] and references therein). The prototype application of these so-called "brute force" Monte Carlo methods is radioactive decay, in which one assumes that all radioactive nuclei are identical, and that during any time interval Δt each nucleus has the same decay probability μ (in s^{-1}) per unit time. The well-known differential equation for this radioactivity process is:

$$\frac{dn}{dt} = -\mu\, n\ , \tag{24}$$

where n represents a continuous variable.

In the case of the Monte Carlo simulations, the differential equation 24 becomes a *difference equation* for the *discrete* variable n:

$$\Delta n = -\mu\, n \Delta t. \tag{25}$$

In this paper, we will apply Monte Carlo methods to the more general equation of the form:

$$\frac{dn}{dt} = -f(n,t)\, n\ , \tag{26}$$

where $f(n,t)$ is a function of the concentration $n(t)$ of trapped electrons at time t. This

differential equation becomes a difference equation during the MC simulations:

$$\Delta n = -f(n,t)\, n\Delta t \ , \tag{27}$$

and the luminescence intensity is evaluated using:

$$I(t) = \frac{\Delta n}{\Delta t} \ . \tag{28}$$

The details of implementing the algorithm have been given recently in Pagonis et al. [13], and only a brief description is provided here. The dimensionless probability P for one trapped electron to recombine within a time interval Δt is $P = f(n)\,\Delta t$, and one chooses a suitable value of Δt so that $P << 1$. In general terms, this simple algorithm proceeds as follows: choose a trapped electron, and a random number r uniformly distributed in the unit interval $0 \leq r \leq 1$ is generated. If $r \leq P$ the trapped electron recombines, otherwise it does not.

In practical terms, a software implementation of equations 27 and 28 proceeds as follows. At time $t = 0$ the initial values are initialized, and the evolution of the system is followed during an appropriate time interval Δt. If the random number $r \leq f(n,t)\,\Delta t$ the electron recombines radiatively, otherwise it does not; all non-recombined remaining electrons in the cluster are tested during each time interval Δt, and several recombination events could take place during each time interval Δt. The value of the remaining electrons in the cluster is updated at the end of each time interval, and the process is continued until there are no electrons left in the cluster. This process is repeated for a large number of MC runs, resulting in the total luminescence intensity given by equation (28).

In order to estimate the stochastic uncertainties in the MC method, the average and variance of a large number of Monte Carlo runs is evaluated. For the simulations presented below, we used the programming environments Mathematica^{TM} and R (R Core Team [29]). The technical details of the implementation in R are beyond the scope of this manuscript and will be presented elsewhere.

5. Results from the MC simulations of stochastic uncertainties

In this section we present the MC results for the stochastic uncertainties in TL, CW-OSL and LM-OSL signals. Subsection 5.1 discusses the results for luminescence models with first-order kinetics, and subsection 5.2 discusses results from the more general OTOR model.

5.1. First-order kinetics: Stochastic uncertainties in TL, CW-OSL and LM-OSL signals

Figure 2 shows a simulation of a TL glow curve consisting of $M = 200$ MC runs for a system of $n_0 = N = 100$ trapped electrons, following the Randall-Wilkins [19] first-order

kinetics equation (2). The thermal parameters of the electron trap are $E = 1\,eV$ and $s = 10^{12}\,s^{-1}$, and the heating rate $\beta = 1\,K/s$.

Panels (a) and (b) in Fig.2 show the results for the electron population $n(T)$ and the TL intensity from 200 MC runs, by using the algorithm described in the previous section. The shaded areas in these two panels indicate the range of the 200 MC runs (i.e. minima and maxima).

Panels (b) and (e) show the standard deviations σ_n and σ_{TL}, which are calculated from the simulations shown in Figs.2ab. The solid lines in panels (b) and (e) are plots of the analytical equations (13) and (21).

Similarly, panels (c) and (f) show the coefficients of variance CV_n and CV_{TL} , and the solid lines in these panels are plots of the analytical equations (14) and (17).

These simulations show good agreement between the stochastic MC runs and the analytical equations previously discussed in Section 3 for pure death stochastic problems.

Figure 3 shows a simulation of a CW-OSL curve consisting of $M = 1000$ MC runs for a system of $N = n_o = 1000$ trapped electrons, following the first-order kinetics equation (4). The optical excitation rate $A_{CW} = 0.04\ s^{-1}$. Panels (b) and (e) show σ_n and σ_{TL} of the CW-OSL process. The solid lines in panels (b) and (e) are plots of the analytical equations (13) and (23). Similarly, panels (c) and (f) show the CV_n and CV_{TL}, and the solid lines in these panels are plots of the analytical equations (14) and (17).

Figure 4 shows a simulation of a LM-OSL curve consisting of $M = 2000$ MC runs for a system of $N = n_o = 1000$ trapped electrons, following the first-order kinetics equation (8). The optical excitation rate $A_{LM} = 0.08\ s^{-1}$ and the maximum excitation time is $P = 220\,s$. Once more, the solid lines in panels (b) through (f) represent the analytical equations given in Sections 2 and 3.

Overall the simulations in Figs. 2, 3 and 4 show good agreement between the stochastic MC runs and the analytical equations, which were previously published for pure death stochastic problems (Allen [25] , Kendall [26]). In all three figures the $CV[\%]$ is a monotonically increasing function of time (or temperature).

In a typical CW-OSL experiment involving quartz, researchers employ the initial portion of the signal (e.g., the first second) in the CW-OSL intensity. By contrast, in typical TL or LM-OSL experiments researchers measure the maximum TL or LM-OSL signal. This difference between experimental protocols means that stochastic uncertainties in CW-OSL signals will be much smaller than the corresponding uncertainties in a TL or LM-OSL signal.

This important result from the simulations is verified in the next subsection, when the simulations are repeated within the more complex OTOR model of luminescence.

5.2. Stochastic uncertainties within the OTOR model

In this section we study the stochastic uncertainties within the OTOR model, which includes the possibility of electrons being retrapped (instead of recombining) during the thermal/optical excitation of the sample. It is important to note that the OTOR model involves nonlinear equations, and therefore there are no analytical solutions available for the coefficients of variation $CV[\%]$.

The two parameters which are varied within the OTOR model are the trap filling ratio n_o/N , and the retrapping ratio R .

Figure 5a shows three different TL glow curves calculated with $R = 10^{-7}, 0.5, 1$ by using equation (9) for the OTOR model. The two curves for $R = 10^{-7}$ and $R = 1$ correspond to first and second order kinetic processes, while the middle curve for $R = 0.5$ can be described empirically as a general order kinetics curve with intermediate order kinetics.

Figure 5b shows simulations of the coefficient of variation CV for TL processes, as a function of the retrapping ratio R which is varied over many orders of magnitude between $R = 10^{-7}$ and $R = 1$. The three curves are evaluated for different values of the total number of particles $n_o = N = 50, 100, 300$. This figure shows that the $CV[\%]$ is practically constant between $R = 10^{-7}$ and $R = 0.1$, and increases slightly for R values between 0.1 and 1, as the kinetics approaches second order.

Figure 6 shows the simulations of a CW-OSL signal in the OTOR model, as a function of the total number of electrons $50 \leq n_o, N \leq 10^4$. The retrapping ratio is kept fixed at $R = 10^{-7}$. As expected in a MC simulation, the stochastic CW-OSL uncertainty decreases as N increases. This makes physical sense, since we expect that the stochastic uncertainties will become negligible as N increases and the behavior of the system approaches the deterministic behavior described by the differential equations approach. Furthermore, the solid line in this figure represents the value $CV = 100/\sqrt{N}$, which one expects for a Poisson distribution. For example, when $N = 10^4$ particles, the $CV[\%]$ value is close to $100/\sqrt{10^4} = 1\%$. Good agreement is once more found with stochastic variation of $CV[\%]$ in the MC simulations and the general expected behavior of a stochastic system.

Figure 7abc shows the simulations of TL, CW-OSL and LM-OSL signals, for different values of the of the total number of particles $n_o = N = 50, 100, 200, 500$. The retrapping ratio is kept fixed at $R = 10^{-7}$.

Figures 8abc show the $CV[\%]$ which are calculated from similar simulations as Figure 7abc, and as functions of the trap filling ratio n_o/N. By comparing the panels in Figure 8, it is clear that the stochastic uncertainty of the maximum TL signal is much larger than the uncertainty of the initial CW-OSL signal. In terms of experimental work, this indicates that the initial CW-OSL signal is much less likely to be affected by the stochastic uncertainties

considered in this paper. The $CV[\%]$ for LM-OSL signals is in-between those for TL and CW-OSL.

This difference between the behavior of the initial CW-OSL signal and the maximum TL signal, is due to the different time dependence of these two stimulation modes. During a CW-OSL experiment the optical excitation rate A is constant and does not depend on the time elapsed from the beginning of the experiment. By contrast, during a TL experiment the thermal excitation rate $s\,exp(-E/kT)$ increases drastically with the time elapsed from the beginning of the experiment.

Figures 5-7 show only the results for cases $n_o = N$ in the OTOR model. However, additional simulations were also considered, in which n_o and N are not equal. The conclusions from these additional simulations are the same as in the case $n_o = N$, so these results are not shown here.

6. Discussion and conclusions

The simulation results in this paper are relevant to two research areas, namely the study of luminescence signals from nanodosimetric luminescent materials, and also in the more specific area of single grain CW-OSL experiments (Wintle and Adamiec [30]).

One of the fundamental questions that this paper attempts to answer by simulation, is under what kind of conditions one can expect stochastic uncertainties to become important during a luminescence dosimetry experiment? The simulations in this paper show that the stochastic uncertainties could become statistically significant when the number of particles participating in the luminescence process is $N = 1000$, or smaller.

Luminescence dosimetry researchers have to take into account several sources of uncertainty, during determination of radiation doses received by a sample (e.g. Anechitei-Deacu et al., [31], Bo Li et al. [32], Bluszcz et al. [33], Adamiec et al. [34], Duller [35], Jacobs et al. [36], Galbraith et al. [37]). The stochastic uncertainties examined in this paper are due to the randomness introduced by the luminescence process itself, and are expected to become important when a small number of particles participates in the production of the luminescence signal. As a numerical example, when one is dealing with a large number of bright luminescent grains larger than 100 μm, these stochastic uncertainties are not expected to influence the precision and accuracy of experimental work, since they vary as the inverse square root of the number of particles participating in the luminescence process. However, recent experimental and modeling work has indicated that these stochastic uncertainties can become important when one is dealing with grain sizes in the range of 1 μm. We now discuss these recently published results.

Polymeris et al., [16] studied the well-known phenomenon of anomalous fading (AF) of luminescence signals in grains of natural Durango apatite. Anomalous fading was found to be ubiquitous for all luminescence signals in this material, and for all grain size fractions. The AF rate for some of these luminescence signals was found to depend on three experimental factors, namely the grain size, the temperature along the glow curve, and on the ball milling time that the samples underwent. On the modeling side, Pagonis and Truong [38] examined possible correlations between the nanocrystal size and the shape and magnitude of TL signals, by using Monte Carlo simulations. These authors showed that in materials for which quantum mechanical tunneling is the dominant recombination mechanism, the TL signals depend on the physical size of the crystal, on the quantum tunneling length, and on the relative concentrations of electrons and positive charges. They also presented new experimental data for Durango apatite samples which underwent ball milling process for different amounts of time. The magnitude and shape of these TL signals depended on the size of the grains in the samples.

Autzen et al. [17] investigated the possibility of charge imbalance in grains of quartz, by using high dose experiments and also by modeling the irradiations using *GEANT4* simulations. For a typical TL/OSL reader and commonly used irradiation dose rates in the laboratory they estimated by simulation that the electron-hole production rate in a single grain disk is of the order of $(81.3 \pm 0.4) \times 10^3$ pairs/Gy. According to this numerical estimate, a sample irradiated with a beta dose of 1 mGy will correspond approximately to N =80 electron-hole pairs. When such a small number of electron-hole pairs is involved in the luminescence process, one would expect that the stochastic uncertainties will become important, and that they will be of similar order of magnitude as other sources of experimental error. This is especially important during single grain quartz experiments.

The second important conclusion from the simulations is that for monotonic luminescence signals (like CW-OSL), one would expect smaller stochastic uncertainties than peak-shaped luminescence signals (like TL and LM-OSL). This is because during CW-OSL experiments researchers typically use only the initial part of the luminescence signal (first 1 second), rather than the complete CW-OSL curve. By contrast, the stochastic error in TL or LM-OSL experiments is much larger, because it would be usually estimated near the peak of the luminescence signal.

The simulations also show that retrapping phenomena most likely have a small effect on the magnitude of the stochastic uncertainty, although they will influence the magnitude of the corresponding luminescence signals. The simulations show that the magnitude of the stochastic uncertainties depends strongly on the degree of trap filling, and that stochastic uncertainties become smaller as one approaches saturation of the dosimetric traps.

The MC method presented in this paper is easily generalized to other types of luminescence signals, and provides a method of estimating the stochastic uncertainties inherent in the luminescence process. Future work in progress is to study these stochastic uncertainties for more complex delocalized transition models like the non-interactive and interactive multitrap models (NMTS and IMTS), and also for localized transitions and quantum tunneling models (Kitis et al. [7]).

7. Acknowledgments

We are grateful to Johannes Friedrich for his initial implementation of the mentioned Monte Carlo methods in R, for which a detailed description will be presented elsewhere. The work by ARD, ER, CL and CS was supported by the project 'ULTIMO: Unifying Luminescence Models of quartz and feldspar' (German Academic Exchange Service) DAAD: Deutscher Akademischer Austauschdienst DAAD PPP USA 2018, ID: 57387041). The work of SK was financed by the LaScArBx, a program supported by the ANR – no. ANR-10-LABX-52 (France).

REFERENCES

References

[1] Chen, R. and McKeever, S.W.S. 1997. Theory of Thermoluminescence and Related Phenomena, World Scientific.

[2] McKeever, S.W.S. , Chen, R., 1997. Luminescence Models Invited Review Paper, Special Issue on Luminescence Dating Radiat. Meas. 27, 625-661.

[3] Bøtter-Jensen, L., McKeever, S.W.S., Wintle,A.G., 2003 Optically Stimulated Luminescence Dosimetry, Elsevier Science B.V.

[4] Pagonis, V., Kitis, G., Furetta, C., 2006. Numerical and Practical Exercises in Thermoluminescence; Springer: New York, NY, USA, 2006; ISBN 0-387-26063-3.

[5] Chen, R. , Pagonis, V., 2011, Thermally and Optically Stimulated Luminescence: A Simulation Approach, Wiley, 2011.

[6] Yukihara, E., McKeever, S.W.S., 2011, Optically stimulated luminescence: fundamentals and applications, (John Wiley Sons Ltd, 2011).

[7] Kitis,G., Polymeris, G.S., Pagonis,V. 2019. Review: Stimulated luminescence emission: From phenomenological models to master analytical equations. Appl. Radiat. Isot. , 153, 108797.

[8] Mandowski, A., Swiatek, J., 1998. Thermoluminescence and trap assemblies—results of Monte Carlo calculations. Radiat. Meas. 29, 415-419.

[9] Mandowski, A.J., 2005. Semi-localized transitions model for Thermoluminescence. Phys. D: Appl. Phys. 38, 17-21.

[10] Mandowski, A., 2006. Calculation and properties of trap structural functions for various spatially correlated systems. Radiat. Prot. Dosim. 119, 85-88.

[11] Mandowski, A., 2008. How to detect trap cluster systems? Radiat. Meas. 43, 167-170.

[12] Kulkarni, R.N., 1994. The development of the Monte Carlo method for the calculation of the thermoluminescence intensity and the thermally stimulated luminescence. Radiat. Prot. Dosim. 51, 95-105.

[13] Pagonis, V., Friedrich, J., Discher, M., Müller-Kirschbaum, A., Schlosser, V., Kreutzer, S. , Chen, R., Schmidt, C., 2019. Excited state luminescence signals from a random distribution of defects: A new Monte Carlo simulation approach for feldspar, J. of Lumin. 207 , 266 - 272.

[14] Swandic, J. R., 1992. Stochastic approach to recombination luminescence with retrapping in the steady state. Phys. Rev. B 45, 622-634.

[15] Swandic, J. R., 1996. Stochastic analysis of multiple-level recombination luminescence and retrapping in the steady state. Phys. Rev. B 53, 2352-2366.

[16] Polymeris, G.S., I.K. Sfampa, I.K., Niora, M., Stefanaki, E.C., Malletzidou, L., Giannoulatou, V. , Pagonis, V. , Kitis, G. 2018. Anomalous fading in TL, OSL and TA – OSL signals of Durango apatite for various grain size fractions; from micro to nano scale. J. of Lumin. 195 , 216–224.

[17] Autzen, M., Murray, A.S. , Guérin, G. , Baly, L., Ankjærgaard, C. , Bailey, M., Jain, M., Buylaert, J.-P. 2018. Luminescence dosimetry: Does charge imbalance matter? , 2018. Radiat. Meas. 120, (2018), 26-32.

[18] Novozhilov, A.S., Karev, G.P., Koonin, E.V. 2006. Biological applications of the theory of birth-and-death processes, Briefings in Bioinformatics, 7, 2006, 70–85. https://doi.org/10.1093/bib/bbk006.

[19] Randall, J. T. , Wilkins, M. H. F. (1945) Phosphorescence and electron traps I. The study of trap distributions. Proc. R. Soc. London 184, 366-389.

[20] Bulur, E., 1996. An alternative technique for optically stimulated (OSL) experiment. Radiat. Meas. 26, 701-709.

[21] Adirovitch, E. I. 1956. La formule de Becquerel et la loi élémentaire du déclin de la luminescence des phosphors crystallins. J. Phys. Rad. 17, 705-707.

[22] Halperin, A. , Braner, A. A. (1960) Evaluation of thermal activation energies from glow curves. Phys. Rev.117, 408-415.

[23] Kitis, G., Vlachos, N.D., 2013. General semi-analytical expressions for TL, OSL and other luminescence stimulation modes derived from the OTOR model using the Lambert W-function. Radiat. Meas. 48, 47-54.

[24] Krishnan, Venkatarama, 2015. Probability and Random Processes, 2nd Edition (Wiley).

[25] Allen, Linda J. S., An introduction to stochastic processes with applications to biology, 2010. (Chapman and Hall/CRC, 2nd edition)

[26] Kendall, David G. On the Generalized Birth-and-Death Process. The Annals of Mathematical Statistics, vol. 19, no. 1, 1948, pp. 1–15. JSTOR, www.jstor.org/stable/2236051.

[27] Landau, D.P. , Binder, K., 2013. A Guide to Monte Carlo Simulations in Statistical Physics, Cambridge University Press, 3rd edition.

[28] Gould H., Tobochnik J. , 1995. An Introduction to Computer Simulation Methods. Applications to Physical Systems, 3ed., Addison-Wesley.

[29] R Core Team, 2019. R: A Language and Environment for Statistical Computing. R Foundation for Statistical Computing, Vienna, Austria. https://r-project.org

[30] Wintle, A.G., Adamiec, G. 2017. Optically stimulated luminescence signals from quartz: A review. Radiat. Meas., 98, 10-33.

[31] Anechitei-Deacu, V. ,Timar-Gabor, A. , Thomsen, K.J., Buylaert, J.-P. , Jain, M., Bailey, M., Murray, A.S. 2018. Single and multi-grain OSL investigations in the high dose range using coarse quartz. Radiat. Meas. 120, 124-130.

[32] Li, B., Jacobs, Z., Roberts, R.G., Galbraith, R., Peng, J. 2017. Variability in quartz OSL signals caused by measurement uncertainties: Problems and solutions, Quat. Geochronol., 41, 11-25.

[33] Bluszcz, A., Adamiec, G., Heer, A.J., 2015. Estimation of equivalent dose and its uncertainty in the OSL SAR protocol when count numbers do not follow a Poisson distribution. Radiat. Meas. 81, 46–54.

[34] Adamiec, G., Heer, A.J., Bluszcz, A., 2012. Statistics of count numbers from a photomultiplier tube and its implications for error estimation. Radiat. Meas. 47, 746–751.

[35] Duller G.A.T., 2012. Improving the accuracy and precision of equivalent doses determined using the optically stimulated luminescence signal from single grains of quartz. Radiat. Meas. 47, 770–777.

[36] Jacobs, Z., Wintle, A.G., Roberts, R.G., Duller, G.A.T., 2008. Equivalent dose distributions from single grains of quartz at Sibudu, South Africa: context, causes and consequences for optical dating of archaeological deposits. J. Archaeol. Science 35, 1808–1820.

[37] Galbraith, R.F., Roberts, R.G., Yoshida, H., 2005. Error variation in OSL palaeodose estimates from single aliquots of quartz: a factorial experiment. Radiat. Meas. 39, 289–307.

[38] Pagonis, V., Truong, P. 2018. Thermoluminescence due to tunneling in nanodosimetric materials: A Monte Carlo study, 2018. Physica B 531 (2018) 171–179.

FIGURE CAPTIONS

Figure 1 Energy level diagram for the OTOR model. The transition p indicates thermal/optical excitation process, A_n and A_m are the retrapping and recombination rates, n_c is the concentration of electrons in the conduction band, and m is the concentration of holes in the recombination center.

Figure 2 Simulation of a first-order TL glow curve consisting of $M = 200$ MC runs for $N = 100$ trapped electrons. The parameters of the electron trap are $E = 1\,eV$ and $s = 10^{12}\ s^{-1}$, and the heating rate $\beta = 1\,K/s$. (a) The electron population $n(T)$ (b) The variance σ_n (c) The coefficient of variation CV_n. Panels (d),(e),(f) show the same quantities for the TL intensity. The shaded areas in the top two panels indicate the minimum and maximum range of the MC runs. The solid lines in the bottom four panels are plots of analytical equations in the text.

Figure 3 Simulation of a CW-OSL curve consisting of $M = 1000$ MC runs and for $N = n_o = 1000$ trapped electrons, following first-order kinetics. The optical excitation rate $A_{CW} = 0.04\ s^{-1}$. The panels correspond to the same quantities shown in Figure 2.

Figure 4 Simulation of a LM-OSL curve using $M = 2000$ MC runs for $N = n_o = 1000$ trapped electrons, following first-order kinetics. The optical excitation rate $A_{LM} = 0.08\ s^{-1}$ and the maximum excitation time is $P = 220\,s$. The panels correspond to the same quantities shown in Figures 1 and 2.

Figure 5 (a) shows three different TL glow curves calculated with $R = 10^{-7}, 0.5, 1$ in the OTOR model. (b) The $CV[\%]$ for TL processes, as a function of the retrapping ratio R between $R = 10^{-7}$ and $R = 1$. The three curves are evaluated for different values of the total number of particles $n_o = N = 50, 100, 300$.

Figure 6 Simulations of a CW-OSL signal in the OTOR model, as a function of the total number of electrons $n_o = N$ and for a fixed retrapping ratio $R = 10^{-7}$. The solid line in this figure represents the curve $CV = 100/\sqrt{N}$ for a Poisson distribution.

Figure 7 Simulations of (a) TL, (b) CW-OSL and (c) LM-OSL signals, as a function of the trap filling ratio n_o/N. The retrapping ratio is kept fixed at $R = 10^{-7}$. The four curves correspond to different values of the total number of particles $N = 50, 100, 200, 500$.

Figure 8 The $CV[\%]$ calculated from the corresponding simulations of Figs. 7abc, shown in the same scale. The stochastic uncertainty of the maximum TL signal in (a) is much

larger than the uncertainty of the initial CW-OSL signal in panel (b), and the $CV[\%]$ for LM-OSL signals is panel (c) lies in-between those for TL and CW-OSL.

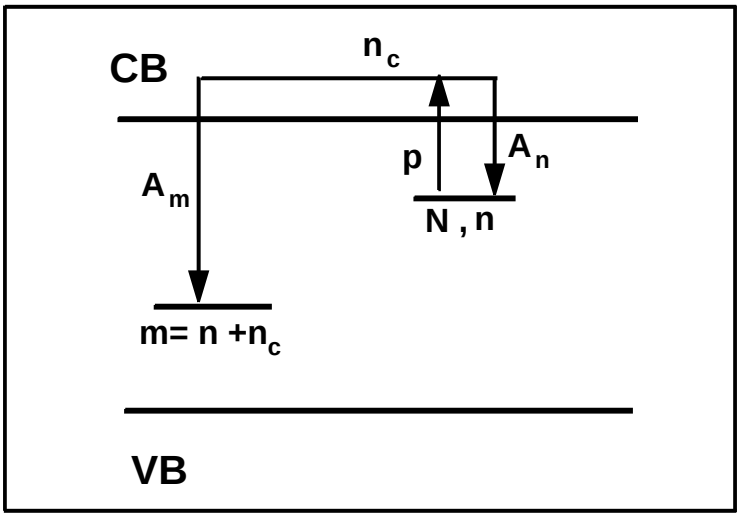

Figure 1: Energy band diagram for the OTOR model. The transition p indicates thermal/optical excitation process, A_n and A_m are the retrapping and recombination rates, $n_c$is the concentration of electrons in the conduction band, and m is the concentration of holes in the recombination center.

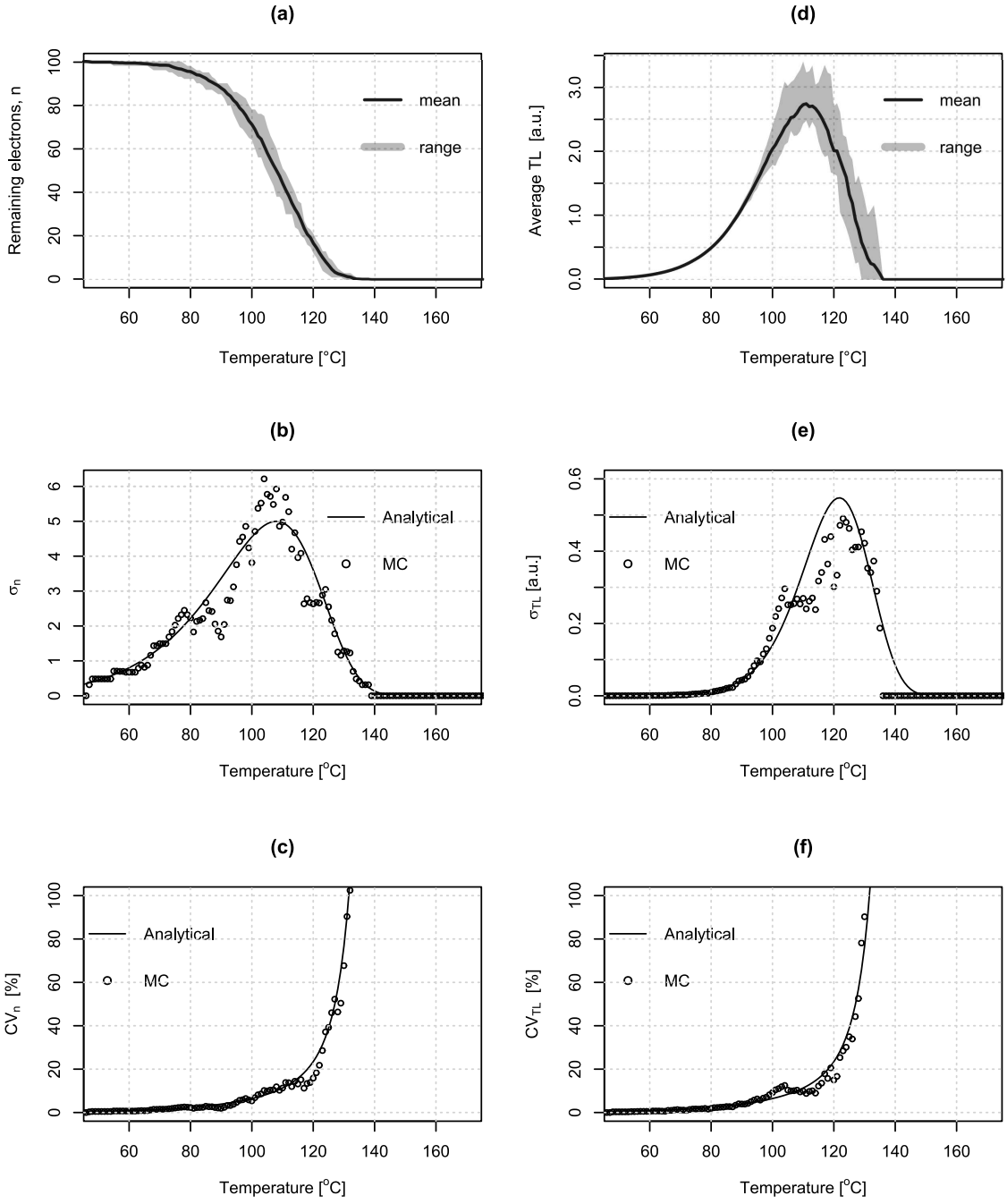

Figure 2: Simulation of a first-order TL glow curve consisting of $M = 200$ MC runs for $N = 100$ trapped electrons. The parameters of the electron trap are $E = 1\,eV$ and $s = 10^{12}\,s^{-1}$, and the heating rate $\beta = 1\,K/s$. (a) The electron population $n(T)$ (b) The variance σ_n (c) The coefficient of variance CV_n. Panels (d),(e),(f) show the same quantities for the TL intensity. The shaded areas in the top two panels indicate the minimum and maximum range of the MC runs. The solid lines in the bottom four panels are plots of analytical equations in the text.

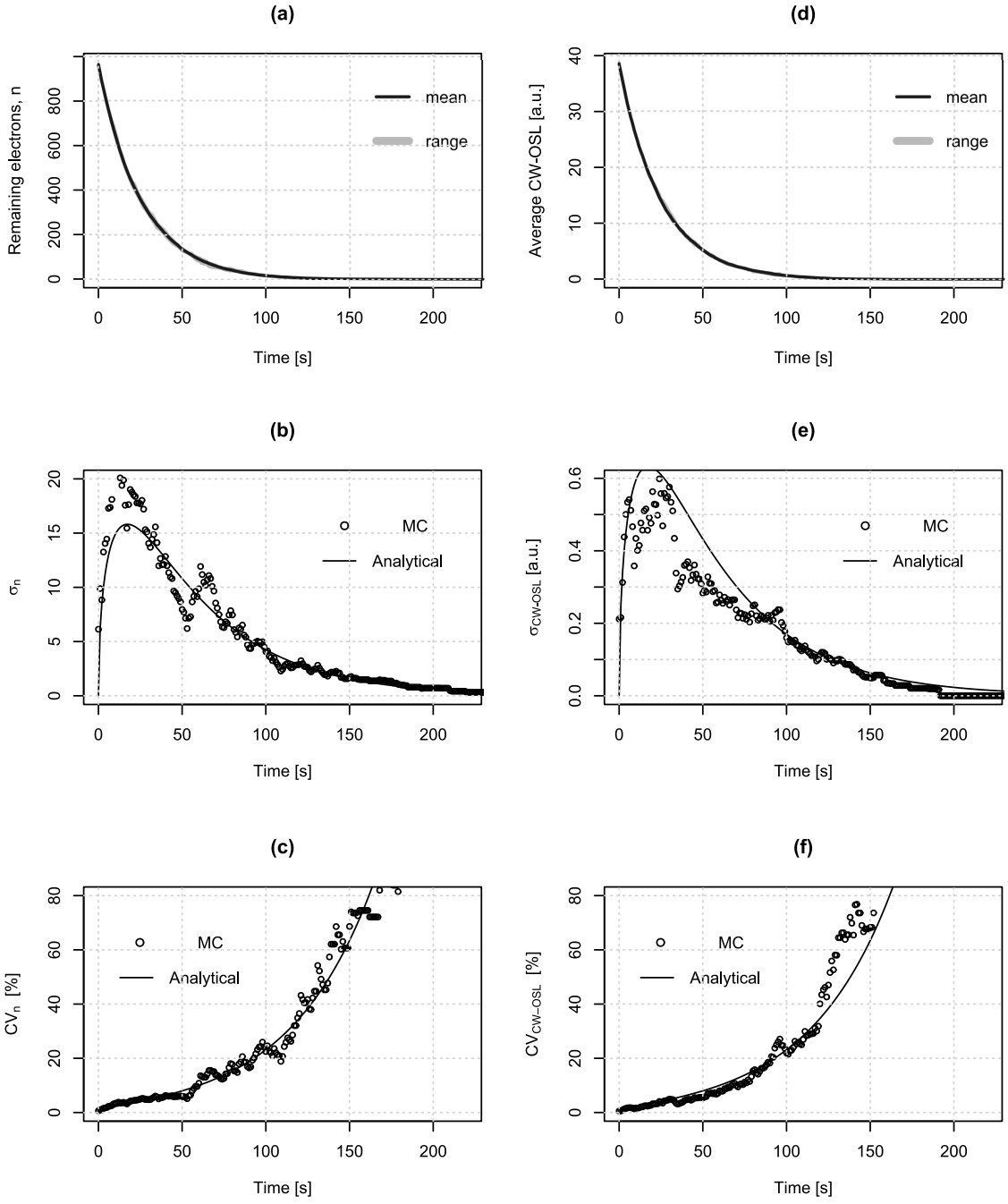

Figure 3: Simulation of a CW-OSL curve consisting of $M = 1000$ MC runs and for $N = n_o = 1000$ trapped electrons, following first-order kinetics. The optical excitation rate $A_{CW} = 0.04\ s^{-1}$. The panels correspond to the same quantities shown in Figure 2.

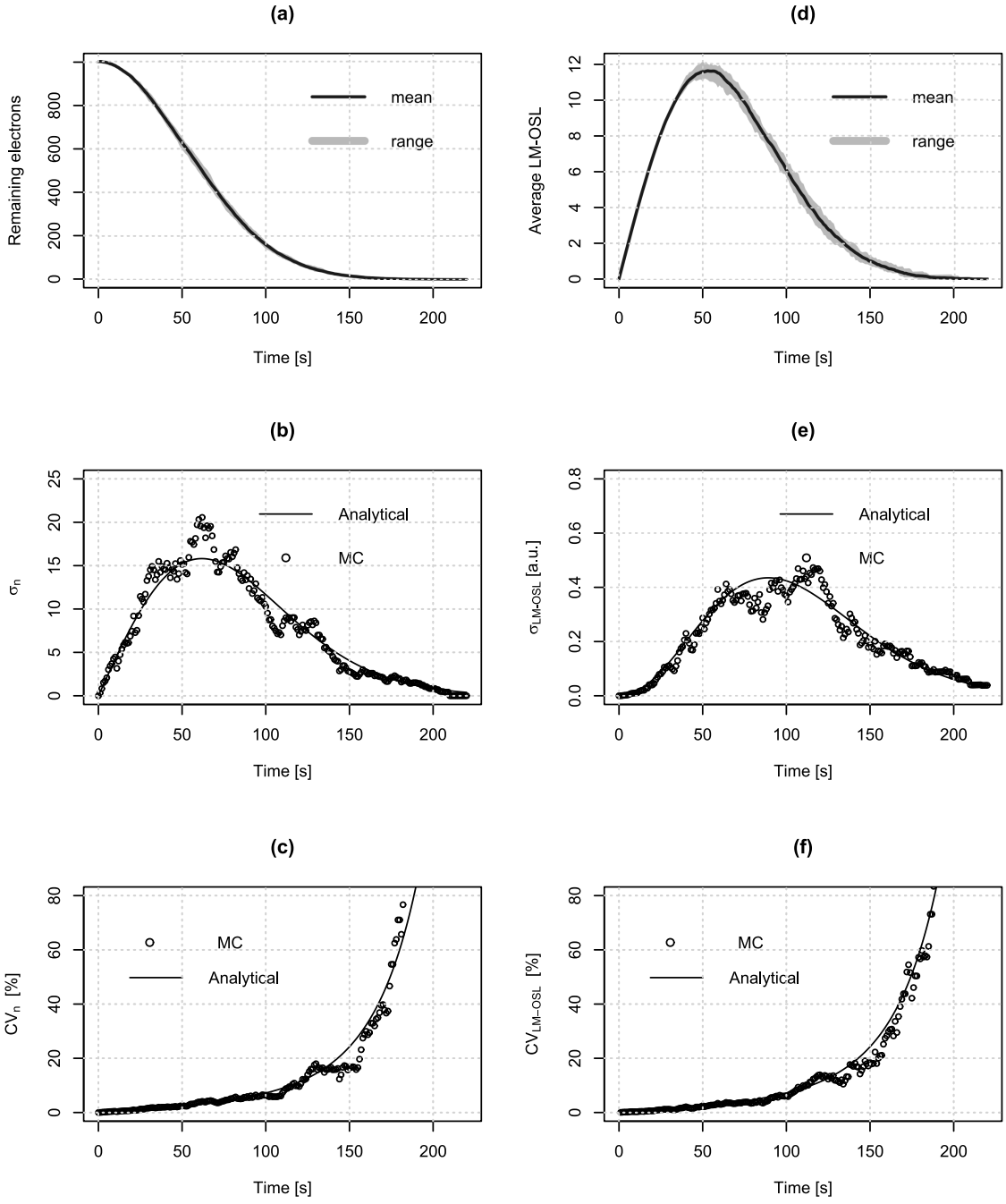

Figure 4: Simulation of a LM-OSL curve using $M = 2000$ MC runs for $N = n_o = 1000$ trapped electrons, following first-order kinetics. The optical excitation rate $A_{LM} = 0.08\ s^{-1}$ and the maximum excitation time is $P = 220\ s$. The panels correspond to the same quantities shown in Figures 1 and 2.

(a)

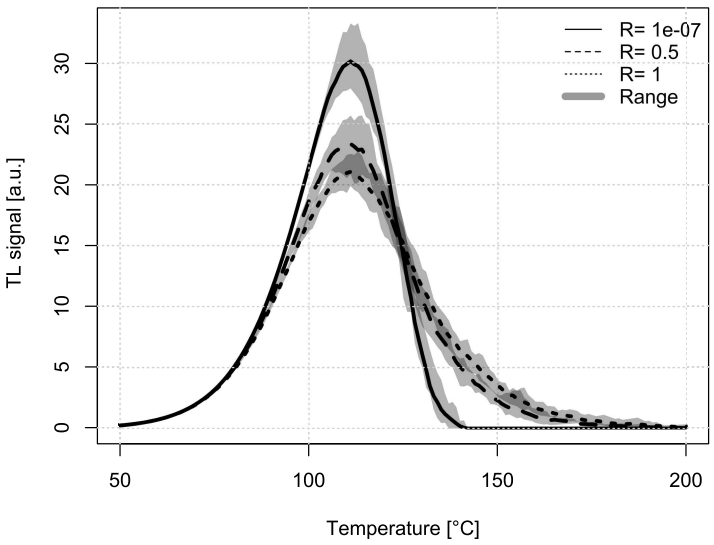

(b)

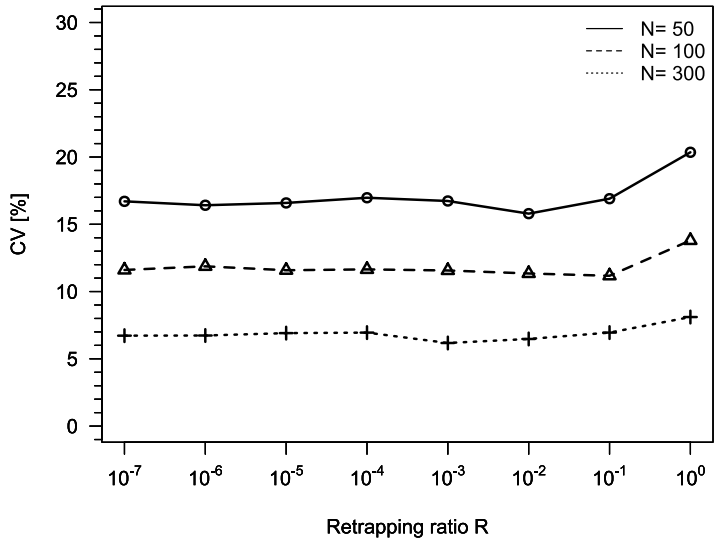

Figure 5: (a) shows three different TL glow curves calculated with $R = 10^{-7}, 0.5, 1$ in the OTOR model. (b) The coefficient of variation $CV[\%]$ for TL processes, as a function of the retrapping ratio R in the range $R = 10^{-7} - 1$. The three curves are evaluated for different values of the total number of particles $n_o = N = 50, 100, 300$.

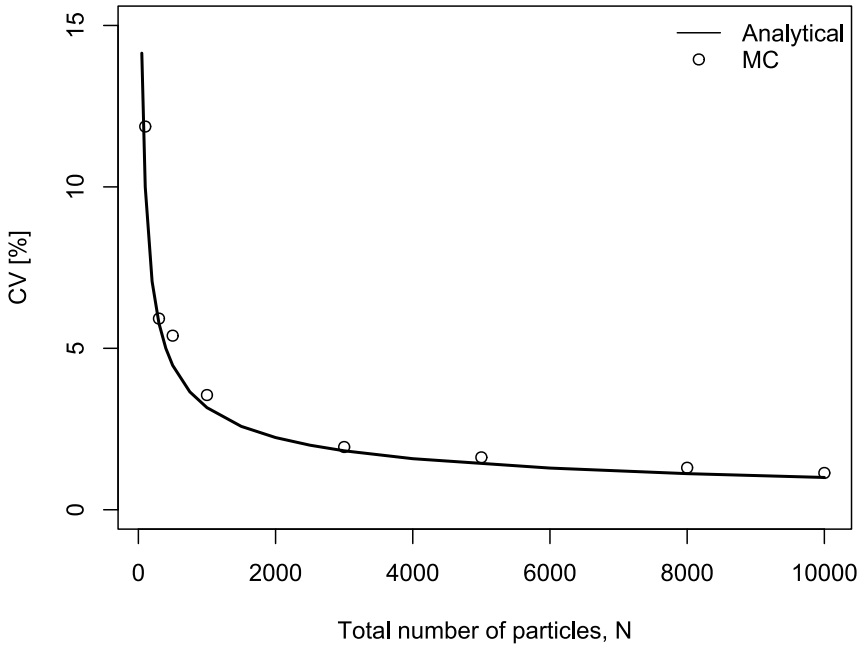

Figure 6: Simulations of a CW-OSL signal in the OTOR model, as a function of the total number of electrons $n_o = N = 50 - 10^4$ and for a fixed retrapping ratio $R = 10^{-7}$. The solid line in this figure represents the curve $CV = 100/\sqrt{N}$ for a Poisson distribution.

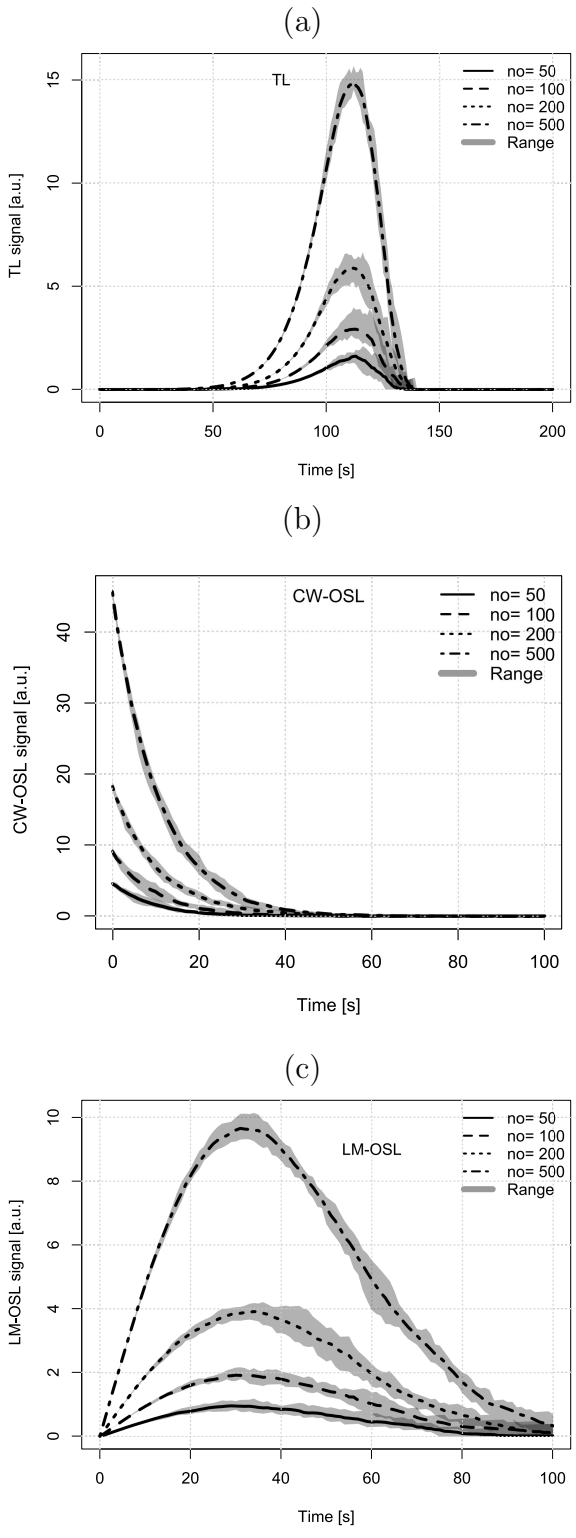

Figure 7: Simulations of (a) TL, (b) CW-OSL and (c) LM-OSL signals, as a function of the number of electrons $n_o = N$. The retrapping ratio is kept fixed at $R = 10^{-7}$. The four curves correspond to different values of the total number of particles $N = 50, 100, 200, 500$.

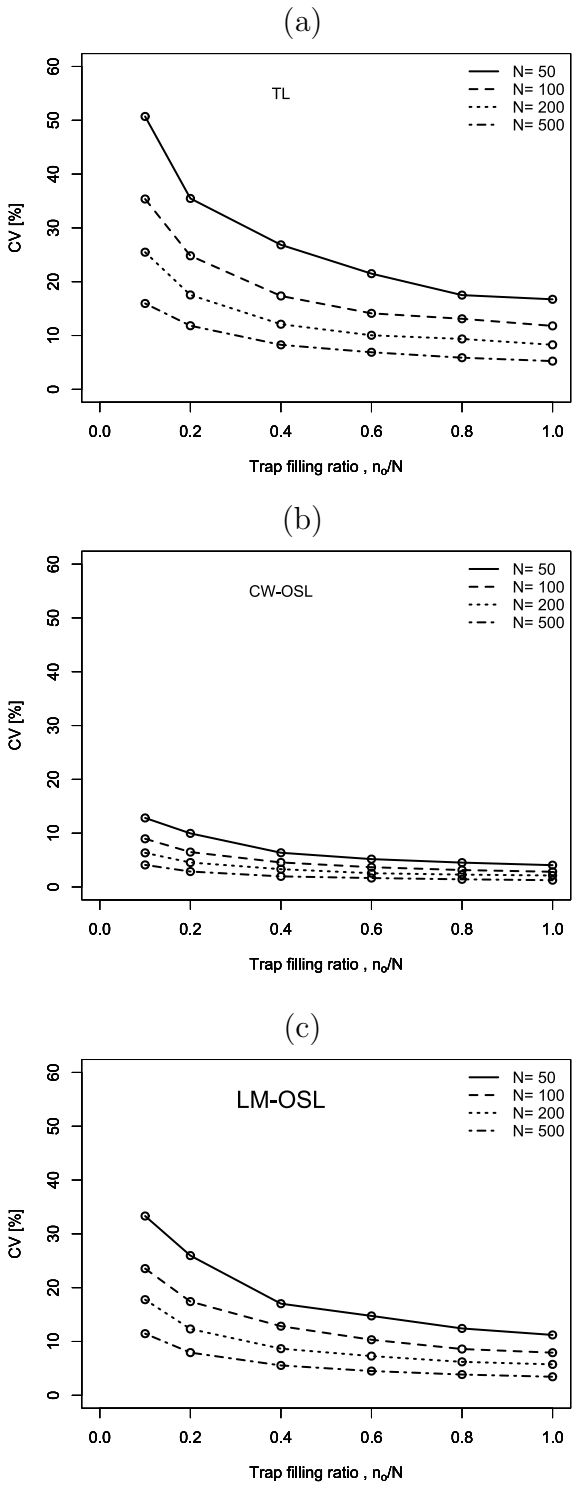

Figure 8: The $CV[\%]$ coefficients calculated from the corresponding simulations of Figure 7abc, shown in the same scale. The stochastic uncertainty of the maximum TL signal in (a) is much larger than the uncertainty of the initial CW-OSL signal in panel (b), and the $CV[\%]$ value for LM-OSL signals is panel (c) lies in-between those for TL and CW-OSL.